Biomass lignin as dispersion to substantially enhance carbon nanotubes thermoelectric converter for energy harvesting

Han Zhang [a], Hui Li[a,*], Wenbo Wang[a], Pengcheng Li[a,*], Siqi Liu[b,c], Ming Yang[d], Chaobin He[b,c,*]

a Hubei Key Laboratory of Plasma Chemistry and Advanced Materials, Hubei Engineering Technology Research Center of Optoelectronic and New Energy Materials, School of Materials Science and Engineering, Wuhan Institute of Technology, Wuhan, 430205, China

b Department of Materials Science & Engineering, National University of Singapore, 9 Engineering Drive 1, 117574, Singapore

c Institute of Materials Research and Engineering, A*STAR (Agency for Science, Technology and Research), 117602, Singapore

d Hubei Integrative Technology and Innovation Center for Advanced Fiberous Materials, 430299, China

Abstract: Carbon nanotubes (CNTs) have attracted much attention as promising thermoelectric materials to harvest waste energy, however the agglomeration between nanotubes greatly limits their application. Despite various dispersants that have been

*Corresponding author. E-mail: mselh@wit.edu.cn (H. Li), msehc@nus.edu.sg (C. He)

devised to enhance the dispersion of CNTs, biomass lignin has been rarely employed to facilitate the dispersion of CNT for enhancing its TE properties. Herein, green lignin was incorporated with CNTs to synergistically improve the dispersion and TE properties of CNTs, in which π-π interactions between the aromatic ring structure of lignin and CNTs, as well as electrostatic charge brought by ionized groups of lignin promote the exfoliation of nanotubes and reduces CNTs entanglement. The well-dispersed structure of CNTs facilitates efficient charge transfer, and thereby enhances the thermoelectric properties. CNTs/lignin composite could reach a maximum power factor of 198.0 μW $m^{-1}K^{-2}$ at a lignin content of 11.8 wt%, which was then raised to 223.1 μW $m^{-1}K^{-2}$ with subsequent partial removal of lignin by alkali immersion treatment, higher than 98.6 μW $m^{-1}K^{-2}$ of pristine CNTs film. Furthermore, the flexible TE device with five pairs of CNTs/lignin and nickel wires generates a high power of 288 nW at ΔT = 30 K, demonstrating potential applications of lignin for sustainable energy harvesting.

Keywords: carbon nanotubes; lignin; dispersion; thermoelectric

1. Introduction

Lignin, the second most abundant natural macromolecule which comprises 30% of the woody biomass, is available in large quantities of approximately 50 million tons per year as a byproduct waste in the paper pulp industry [1-4]. With the impressive merits of renewable, unique structure, and biocompatibility, lignin has been considered as a promising sustainable alternative to substitute fossil fuel resources for practical

applications [5, 6]. Despite great progress has been achieved in the conversion of lignin to various high-value-added products, more efforts are still needed to expand their use in high-value-added applications, especially thermoelectric (TE) technology. Recently, with the crisis of fossil fuel depletion and environmental pollution, TE technology has attracted enormous attention due to its unique ability to directly convert waste heat into electrical energy [7-10]. The thermoelectric properties of TE materials are usually characterized by $ZT=S^2\sigma T/\kappa$, where S is Seebeck coefficient, σ is electrical conductivity, κ is thermal conductivity and T is absolute temperature, in which $S^2\sigma$ defined as power factor (PF) is often employed to evaluate the TE performance [11-13]. Currently, carbon nanotubes (CNTs) are particularly attractive for TE application owing to their unique merits of good flexibility, high carrier mobility, chemical inert, and high strength [14-16].

Due to the high aspect ratio and strong Van der Waals forces between nanotubes, the CNTs bundles are prone to tangle with each other and aggregate, leading to agglomeration of CNTs and deteriorated carrier transport [17]. Such aggregations result in inferior mechanical and electrical properties, greatly impeding their practical applications, especially in TE conversion. Therefore, good dispersion of CNTs is a prerequisite for better electrical conductivity, and many approaches have been devoted to enhancing the dispersion of CNTs bundles [11]. Mechanical methods (such as ultrasound, stirring, ball milling, etc.) and chemical functionalization consisting of covalent functionalization and noncovalent functionalization are commonly employed strategies to disperse CNTs [18-21]. In particular, the noncovalent functionalization

method in which the dispersants can wrap CNTs through strong noncovalent interactions, has attracted significant interest due to the advantages of facile procedure and preservation of the intrinsic electronic structure [22-25]. In recent years, varied dispersants have been employed to promote the dispersion of CNTs, and aromatic chemicals are preferentially attractive due to the presence of π-π interactions between the aromatic groups of compounds and CNTs, which facilitate the dispersion of CNTs and enhance their thermoelectric properties [26-29]. Our group investigated the TE performance of SWCNT film by the dispersant of poly(styrene sulfonic acid) (PSSH) and sequential base treatment [30]. Ascribing to π-π interactions between the PSSH and CNTs and the doping effect of PSSH, PSSH is prone to absorb on the surface of CNTs, which effectively improves the dispersibility of CNTs, giving rise to enhanced electrical conductivity and power factor up to 117.7 μW $m^{-1}K^{-2}$. However, the excessive addition of surfactant would also deteriorate carrier transport and lead to a decrease in electrical properties [31-33]. Even though various studies highlight the dispersing effect of additives for CNTs, the harmful petroleum-based chemicals need to be minimized due to the related environmental issues, and sustainable eco-friendly alternatives are highly demanded for exfoliating CNTs bundles and boosting the TE performance of CNTs films.

Renewable resource lignin has been investigated as one of the most promising dispersants to disperse CNTs. The unique structure with an abundance of aromatic groups enables lignin to form enhanced interfacial interactions with nanotubes through π-π interactions, leading to stable CNTs dispersions[34, 35]. Dichiara *et al.* [36]

investigated the dispersing ability of lignin to prepare aqueous CNTs suspensions. Compared with other typical petroleum-based surfactants (SDS and CTAB), lignin was more effective in dispersing CNTs and stabilizing CNTs dispersions, ascribing to the aromatic structures to promoting π-π interactions with CNTs and steric stabilization. Lu *et al.* [37] reported lignin-assisted direct exfoliation of graphite to graphene using alkali lignin as a surfactant and stabilizer, attributing to π-π interaction between the graphene and lignin and the electrostatic repulsion between negatively charged lignin. Consequently, high-concentration aqueous graphene dispersions were obtained and the resultant graphene films exhibited good electrical conductivity (26 S cm^{-1}). These results demonstrate the feasibility of using lignin as an effective dispersant to disperse CNTs and enhance conductivity. Recently, C, Mario *et al.*[38] developed lignin-doped CNTs yarns (CNTY) by immersing CNTs yarns in a lignin solution, which showed a simultaneous increase in conductivity and Seebeck coefficient. They speculated that the strong π-π interactions between lignin and CNTs promote the formation of an interconnected nanostructure with improved conductivity, and carrier filtering effect between CNTY and lignin contributed to the enhanced *S*. With properly modulating lignin content, the power factor of CNTY/lignin yarns was significantly increased to 132.2 μW m^{-1} K^{-2}, higher than 56 μW m^{-1} K^{-2} of pristine CNTs yarns. These results show the potential application of lignin in electronic devices and renewable energy harvesting systems, while biomass lignin has been rarely employed to facilitate the dispersion of CNT for enhancing its TE properties.

Herein, we report the boosting TE properties of CNTs by biomass lignin dispersing

and sequential base treatment. Lignin served as an effective dispersant to improve the dispersion of CNTs and thereby construct uniform conductive networks to facilitate carrier transport. Considering the intrinsic insulative property of lignin, CNTs/lignin composite films were further base treated to remove extra lignin. By optimizing the content of lignin and durations of base treatment, a maximum power factor of 223.1 $\mu W\ m^{-1}\ K^{-2}$ was achieved for the CNTs/lignin composite film. Moreover, the mechanism behind the enhanced TE performance was investigated by SEM, Raman, FTIR, and Hall measurements. Finally, a flexible TEG consisting of 5 legs of CNTs/lignin films was fabricated, which delivered a remarkably high output power of 288 nW and voltage of 8.7 mV at ΔT of 30 K. This study not only paves the way for improving the dispersibility and TE performance of CNTs by renewable lignin, but also highlights the potential application of lignin as a promising green alternative to traditional petrochemical-based dispersant in sustainable energy harvesting.

2. Experimental

2.1 Materials.

Single-walled carbon nanotubes (CNTs) (purity>95 wt%, TNSAR type, length of 5 - 30 μm, and outer diameter less than 2 nm) were purchased from Chengdu Organic Chemicals Co. Ltd., China. Lignin (Mn = 3600) was obtained from Sigma-Aldrich and was used after acid washing according to the literature [2, 39]. Ammonium hydroxide ($NH_3 \cdot H_2O$) was purchased from Sinopharm Chemical Reagent Co. Ltd.

2.2 Preparation procedures of CNTs/lignin films

Lignin was first dissolved in 0.5 M ammonia hydroxide to prepare a lignin solution

with a concentration of 5 mg mL^{-1}. After that, a varied amount of CNTs was dispersed in 2 mL lignin solution with the aid of an ultrasonic probe dismembrator (SEIENTZ JY92-IIN) for 5 minutes. Then the CNTs dispersion was further stirred by a vortex mixer for 5 minutes. Finally, the resultant dispersion was drop-casted on glass substrates (pre-cleaned with deionized water and ethanol), followed by drying on a hot plate at 60 ℃ to yield the CNTs/lignin films. The percentage of lignin in the composite film was varied from 0 to 23.1 wt%. Furthermore, CNTs films without lignin were also prepared according to the above-mentioned process for comparison.

As for the base treatment, the as-prepared CNTs/lignin films were immersed in 0.5 M ammonia solution for various minutes in ambient air. Subsequently, the sample was removed from the ammonia solution and washed with deionized water. The treated films were finally dried on a hot plate at 60 ℃ for 5 h to generate the CNTs/lignin-A films.

2.3 Fabrication of thermoelectric device

The flexible TE device was fabricated by combining five treated CNTs/lignin films with a dimension of 25 mm (length) × 6mm (width) × 8 μm (thickness) and nickel wires. The film and nickel wire were assembled alternately and silver coating was employed on the contact area between nickel wire and composite film to reduce contact resistance. Besides, copper wires were connected to both ends of the TE device to deliver electricity. After that, the assembled films were sealed in PET to fabricate flexible thermoelectric devices.

2.4 Characterization

The microscopic morphology of the CNTs/lignin film was observed by Scanning Electron Microscopy (SEM, Seizz Sigma 300). FTIR spectra were conducted using PerkinElmer FT-IR Spectrometer. Raman measurement was recorded with DXR Raman spectrometer (American Thermo Electron). UV-vis absorption spectra were measured with a PerkinElmer Lambda 35 UV-vis spectrometer. The carrier concentration and carrier mobility of the films were measured using a Hall effect measurement system under a constant magnetic field (Pasic-Hall HT50, Precision Systems Industrial Ltd., China). The composite dispersion was cast on a rectangular glass substrate with a dimension of 1.25 × 1.25 cm^2 for the measurement of electrical conductivity (σ), $\sigma = 1/(R_S d)$, which was calculated by the van der Pauw four-probe technique. The Rs is the sheet resistance of thin films, and d is the film thickness, which was collected using a Bruker Dektak XT stylus surface profiler. The composite solution was cast on a rectangular glass substrate with a dimension of 1.25 × 2.5 cm^2 for the characterization of Seebeck coefficient, which was performed via a home-built system [40]. The film was secured on the Peltier device as the hot side and the cold side was kept under atmospheric conditions. The temperature on the hot side was controlled using a power supply to generate the temperature gradient (ΔT), which was collected by type-T thermocouples. The heat-induced TE voltage (ΔV) was measured with a Keithley 2000 multimeter. The Seebeck coefficient (S) was identified as the slope of linear fitting of $\Delta V/\Delta T$. As for the TE device, the output voltage (V) was collected using Keithley 2000 multimeter. The electrical conductivity and Seebeck coefficient with different temperatures were measured using a TE parameter test system (Namicro-IV).

A Laser thermal conductivity analyzer (NETZSCH LFA467) was used to measure the in-plane thermal diffusivity (α) of the composite film, and the heat capacity (C_p) was assessed with a differential scanning calorimeter (METTLER TOLEDO DSC 3). The formula of $\kappa = \rho\alpha C_p$ was used to calculate the thermal conductivity (κ), where the density (ρ) of the film was determined through its mass and volume. At the temperature gradient of 30 K, various load resistances (R) were connected to the thermoelectric devices, and the resultant output voltage was recorded to calculate output power.

3. Results and Discussion

3.1 Microstructure of CNTs/lignin *composites*

With the existence of Van der Waals force, CNTs tend to be entangled with each other to form large agglomerates when they are dispersed in solution. Notably, the CNTs bundles would form heterogeneous dispersion, and tend to self-aggregate and pack into nodules during the casting process, yielding a packed globular structure with large aggregates (Fig. 1a and 1b). In contrast to pure CNTs, lignin enables the de-bundling of CNTs aggregates and thus promotes the dispersion of CNTs in the solution to achieve stable CNTs suspension, which could remain uniform for a long time. Furthermore, the dispersibility of CNTs in the composite dispersions was gradually increased with increasing lignin concentration. The lignin-dispersed CNTs film exhibited a relatively uniform surface without obvious aggregations. In addition, the effects of lignin and various lignin contents on the distribution of CNTs in CNTs/lignin films were also studied by SEM analysis. For pristine CNTs film (Fig. 1c-e), multiple CNTs were clustered together, forming thicker CNTs bundles and large aggregates. Moreover, it

showed a wide distribution of CNTs bundle diameters and the average bundle diameter was 224 nm, indicating poor dispersion of CNTs without dispersant. In contrast to large bundles of pure CNTs film, a more uniform well-distributed CNTs with smaller bundle diameter was observed for CNTs/lignin film. With the addition of lignin, SEM images showed that the surface of the composite film was relatively smooth and CNTs bundles were randomly distributed to form an interconnected network. As shown in Fig. 1f-h, the diameter of the CNTs bundles was calculated to be 167 nm for CNTs/lignin films with a lignin content of 11.8 wt%. When lignin content was further increased to 23.1 wt%, CNTs bundles were well isolated and the diameter of CNTs bundles was monotonically decreased to 107 nm, only one-half of that of the initial CNTs film. These results demonstrate that the incorporation of lignin significantly promotes the dispersibility of CNTs in the composite film, which can be explained by the wrapping of lignin around CNTs to exfoliate the CNTs bundles [41]. It is beneficial for the formation of an interconnected conductive CNTs network to decrease resistance of adjacent CNTs junctions and facilitate carrier transportation, contributing to enhanced electrical conductivity. In addition, the morphology of 11.8 wt% CNTs/lignin film treated with alkali solution was also investigated, and no obvious change was observed compared to as-prepared CNTs/lignin film, suggesting that alkali treatment does not destroy the already formed structure of the CNTs.

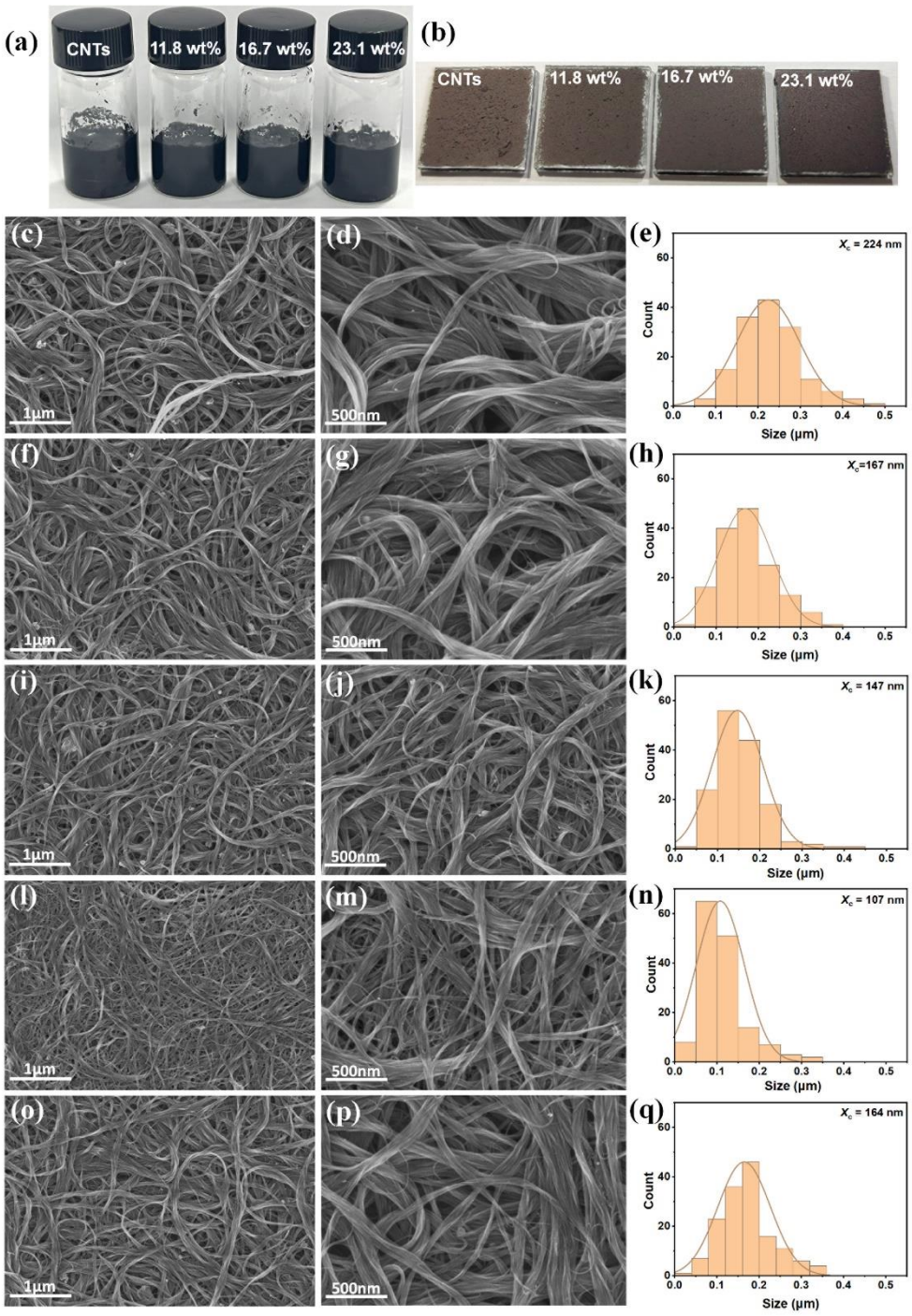

Fig. 1. Comparison of CNTs composite dispersions (a) and films (b) with different lignin contents; SEM images of CNTs/lignin composite films and their statistical results of CNTs beam diameter with different lignin contents (c-e: 0 wt%; f-h: 11.8 wt%; i-k: 16.7 wt%; l-n: 23.1 wt%); (o-q) SEM images of the 11.8 wt% CNTs/lignin-A film with alkaline treatment for 1 min.

Fig. 2a shows the FTIR spectra of CNTs/lignin composite films with different lignin contents, pristine CNT and lignin were also included for comparison. Pure lignin exhibited characterized bands at 1722 and 1630 cm^{-1} which are attributed to unconjugated carbonyl groups and conjugated carbonyl groups, respectively [42-44]. Moreover, the bands at 1538, 1479, and 1440 cm^{-1} were observed in the spectra which are assigned to aromatic skeleton vibrations [45]. With the addition of lignin, an additional band at 1630 cm^{-1} appeared in the spectra of CNTs/lignin composite film in comparison to pure CNTs, and the peak became more pronounced with increasing lignin content to 23. 1 wt%, revealing that more lignin was incorporated to CNTs matrix. Moreover, the band located at 1464 cm^{-1} for pristine CNTs, was shifted to a lower frequency for CNTs/lignin composite, indicating interactions between CNTs and lignin through aromatic skeleton vibrations [38]. The interactions could be further confirmed by Raman spectra. Fig. 2d shows the Raman spectra of CNTs/lignin composite films, pristine CNTs, and pure lignin. The Raman spectrum of the pristine CNTs showed two characteristic peaks at 1590 cm^{-1} (G band) and 1340 cm^{-1} (D band). Generally, the G band is attributed to the in-plane stretching vibrations of sp^2 hybridized carbon atoms, and the D band originates from defects in the nanotube lattice [46-48]. From the partial magnification of the spectra (Fig. 2e), the G peak of CNTs was gradually shifted to higher frequency with increasing lignin content. With lignin concertation of 23.1 wt%, the G peak of CNTs was shifted to 1593 cm^{-1}, suggesting π-π interactions between lignin and carbon nanotubes through aromatic ring structures [49]. With abundant aromatic groups, lignin is prone to tightly bound with CNTs through π-π interactions.

The wrapping of CNTs with lignin facilitates the exfoliating of CNTs bundles and reduces agglomeration, thereby promoting the dispersibility of CNTs to form a uniform conductive network [50].

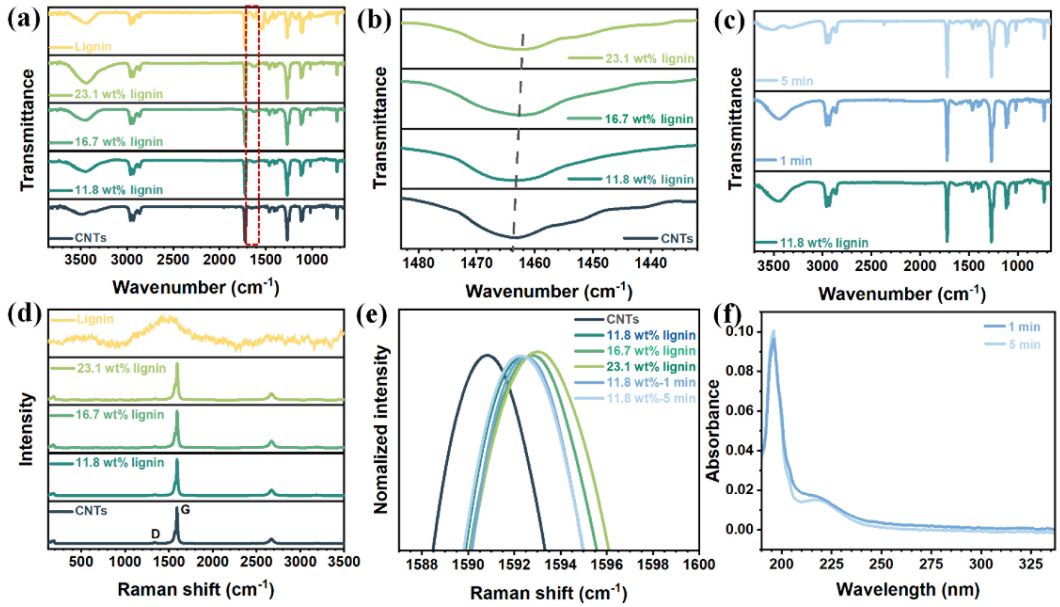

Fig. 2. (a) FTIR spectra of CNTs/lignin composite films with different lignin contents, pure CNTs, and lignin; (b) Magnification of the FTIR spectra between 1483 cm^{-1} and 1432 cm^{-1}; (c) FTIR spectra of 11.8 wt% CNTs/lignin film with alkaline treatment for different time; (d) Raman spectra of CNTs/lignin composite films with different lignin contents, pure CNTs, and pure lignin; (e) Magnification of Raman spectra with range of 1587 cm^{-1}-1600 cm^{-1}; (f) UV-vis spectra of soaked ammonia solutions of 11.8 wt% CNTs/lignin films.

The effect of base treatment on the structure of 11.8 wt% CNTs/lignin film was investigated by FTIR, Raman, and UV-vis spectra. Upon soaking the composite film in ammonia, the intensity of the peak at 1630 cm^{-1} assigned to the conjugated carbonyl group of lignin, decreased compared to the untreated CNTs/lignin film. This suggests

the effective removal of lignin from composite films. Fig. 2c showed that the band located at 1462 cm^{-1} was not blue-shifted after soaking treatment, implying that the interactions between lignin and CNTs remained in the based treated films. Moreover, the G band of the composite film was not displaced back either, which was still located at 1592 cm^{-1}, further confirming the existence of π-π interactions and residual lignin in the composite film even subject to alkali treatment (Fig. 2e). The removal amount of lignin by soaking treatment was calculated by UV-vis spectrum, as shown in Fig. 2f. The soaking solutions of 11.8 wt% CNTs/lignin films for 1 min and 5 min were characterized, and the peak intensity at 200 nm was slightly enhanced with increasing the soaking time. Furthermore, the peak intensity at 200 nm was used for calculating the concentration of lignin (Fig. S1.) [51, 52], and the lignin washed away by ammonia immersion was about 9.2 wt% for 1 min and 10.0 wt% for 5 min. These results demonstrate the partial removal of lignin through ammonia treatment.

3.2 Thermoelectric performance of CNTs/lignin composite films

The TE properties of CNTs/lignin composite films with various lignin contents were investigated and shown in Fig. 3a and b. As shown in Fig. 3a, both the electrical conductivity and Seebeck coefficient showed an increasing and then decreasing trend with an increase of lignin content. As increasing lignin content to 11.8 wt%, CNTs/lignin films reached remarkable improvements in their electrical conductivity and Seebeck coefficient (993 S cm^{-1} and 44.7 μV K^{-1}, respectively). The increased conductivity is mainly attributed to the abundance of aromatic and ionized groups in lignin, which facilitates the dispersion of carbon nanotubes to form a uniformly

interconnected conductive network. As shown in Fig. 3g, since lignin has both hydrophilic hydroxyl functional groups and hydrophobic aromatic chain segments, its amphiphilicity and particular aromatic structure make it better adsorbed and interacted on the surface of carbon nanotubes through π-π interactions. The large three-dimensional mesh structure of lignin generates spatial site resistance, which promotes the stripping of carbon nanotubes under ultrasound. Moreover, the electrostatic charge brought by ionized groups of lignin enables carbon nanotubes charged through the absorption of lignin, which effectively avoids agglomeration of carbon nanotubes by electrostatic repulsion. Therefore, with the presence of lignin, CNTs which were originally agglomerated together become well dispersed with reduced entanglement, producing more uniform conductive pathways. The uniform interconnected CNTs network could effectively reduce energy barriers between nanotube junctions and facilitate carrier transport, giving rise to improved carrier mobility and electrical conductivity (Fig. 3c). On the other hand, the work functions of CNTs and lignin are 5.26 eV and 3.97 eV, respectively, and an energy barrier of 1.29 eV is formed at CNTs/lignin interfaces (as shown in Supporting information as Fig. S2.). Probably ascribing to an energy filtering effect between CNTs and lignin, in which low-energy carriers would be filtered out and high-energy carriers were preferentially passed through, carrier concentration was gradually decreased, contributing to an increased Seebeck coefficient [38, 53-55]. Consequently, the electrical conductivity and Seebeck coefficient of CNTs/lignin composite film were improved synergistically at low lignin content. When further increasing the lignin content to higher than 11.8 wt%, the

electrical conductivity and Seebeck coefficient were simultaneously decreased, probably attributing to the excess accumulation of intrinsic insulative lignin. Although the CNTs bundles were well distributed with small bundle diameters, the excess lignin wrapped on the surface of CNTs served as insulating domains to deteriorate interconnected conductive pathways and impede carrier transport, leading to inferior TE properties. Therefore, a maximum power factor of 198.4 μW $m^{-1}K^{-2}$ was achieved with a lignin content of 11.8 wt%, higher than 98.6 μW $m^{-1}K^{-2}$ of pure CNTs film. Notably, this result demonstrates the contribution of lignin dispersant that synergistically boosts the electrical conductivity and Seebeck coefficient of CNTs.

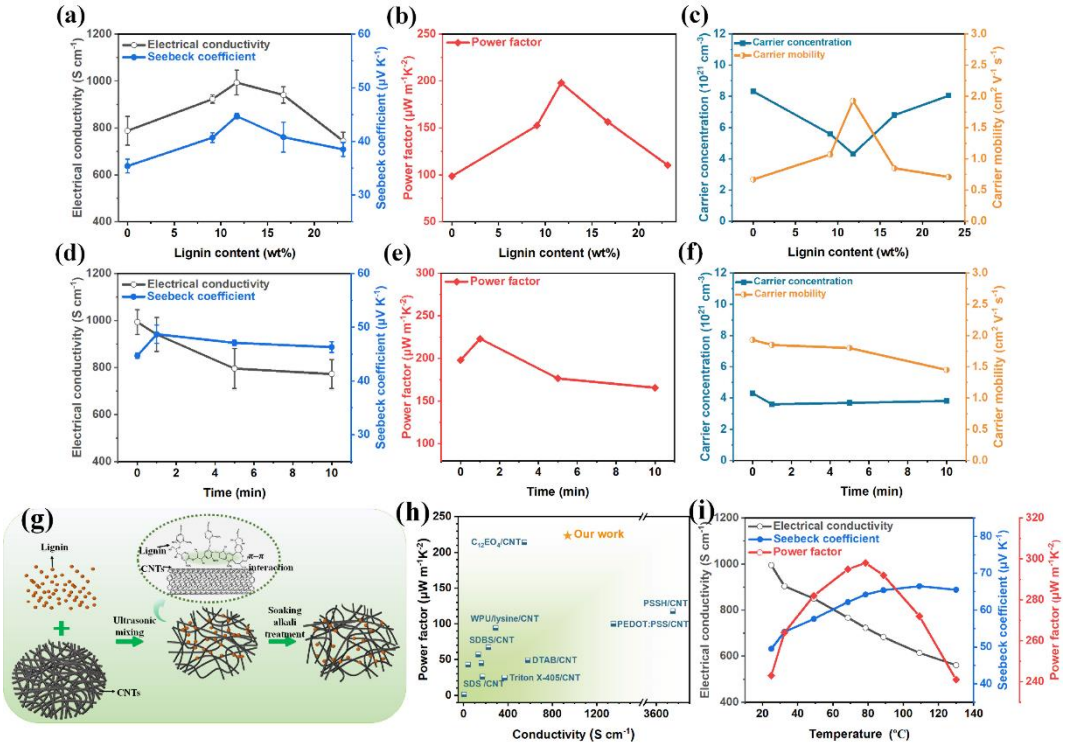

Fig. 3. (a-c) TE properties, carrier concentration and carrier mobility of CNTs/lignin composite films with different lignin contents; (d-f) TE properties, carrier concentration and carrier mobility of the 11.8 wt% CNTs/lignin film subject to alkaline treatment for different times; (g) Schematic diagram of lignin dispersed CNTs films; (h) Comparison

of CNTs TE films summarized from literature, our work was included and noted with orange star; (i) Temperature-dependent thermoelectric parameters of 11.8 wt% CNTs/lignin -A film.

Subsequently, the 11.8 wt% CNTs/lignin films were post-treated by alkali soaking, and the effect of alkali post-treatment on the thermoelectric properties of CNTs/lignin films was investigated as shown in Fig. 3(d-f). With increasing the immersion duration, the electrical conductivity was gradually decreased, mainly ascribing to the partial removal of lignin as confirmed by FTIR and UV-vis results. It is possible that the films become looser and porous due to the removal of the lignin phase, leading to deteriorated carrier concentration and mobility. As the immersion time increased, Seebeck coefficient was increased at first and then almost saturated with further increasing soaking durations. Ultimately, CNTs/lignin composite film reached an optimal power factor of 223.1 μW m^{-1} K^{-2} by immersing in an alkali solution for 1 min, higher than most values of previously reported CNTs films [41, 47, 56-62], as shown in Fig. 3h. Considering the in-plane thermal conductivity (κ) of the 11.8 wt% CNTs/lignin-A film (157.4 W m^{-1} K^{-1}), ZT of 4.3×10^{-4} was achieved. Furthermore, the CNTs/lignin composite film exhibited superior mechanical properties, which is beneficial for practical applications (Fig. S3.).

Subsequently, the temperature-dependent TE properties of 11.8 wt% CNTs/lignin-A film from room temperature to 130 °C under vacuum condition were shown in Fig. 3i. The electrical conductivity decreased monotonically with an increase of temperature,

indicating a metallic-like conducting behavior of the film. The deteriorated electric conductivity was probably attributed to the morphology expansion during heating, which results in an inferior conductive path for charge carrier transportation [63, 64]. Seebeck coefficient of the film was increased with increasing temperature. The enhanced Seebeck coefficient could be ascribed to the slight morphology expansion during heating, which causes an increase of the energy barrier between CNTs junctions and thus decreased carrier concentration [65, 66]. Consequently, a maximum PF of 298.4 μW m^{-1} K^{-2} was achieved at 80 °C, demonstrating the potential application of CNTs/lignin composite films for practical thermoelectric conversion.

To investigate the practical application of CNTs/lignin films on wearable energy harvesting, a flexible thermoelectric device was assembled by connecting five legs of P (CNTs/lignin-A film)-N (nickel wire) modules in series (Fig. 4a). Fig. 4 (b) shows the open-circuit voltage of TEG with varied temperature gradients. With the increase of temperature difference from 5 K to 30 K, the open-circuit voltage of the flexible thermoelectric device increased linearly from 1.3 mV to 8.7 mV. At ΔT = 30 K, the output voltage was almost linearly increased with the decrease of current, and the output power exhibited a typical parabolic curve relationship as a function of current. The TEG generated a maximum output power of 288 nW at the load resistance of 68 Ω, which is close to the internal resistance of the module (69 Ω). The output performance of thermoelectric devices prepared from CNTs films is superior to most previously reported CNTs-based TE devices [67-69].

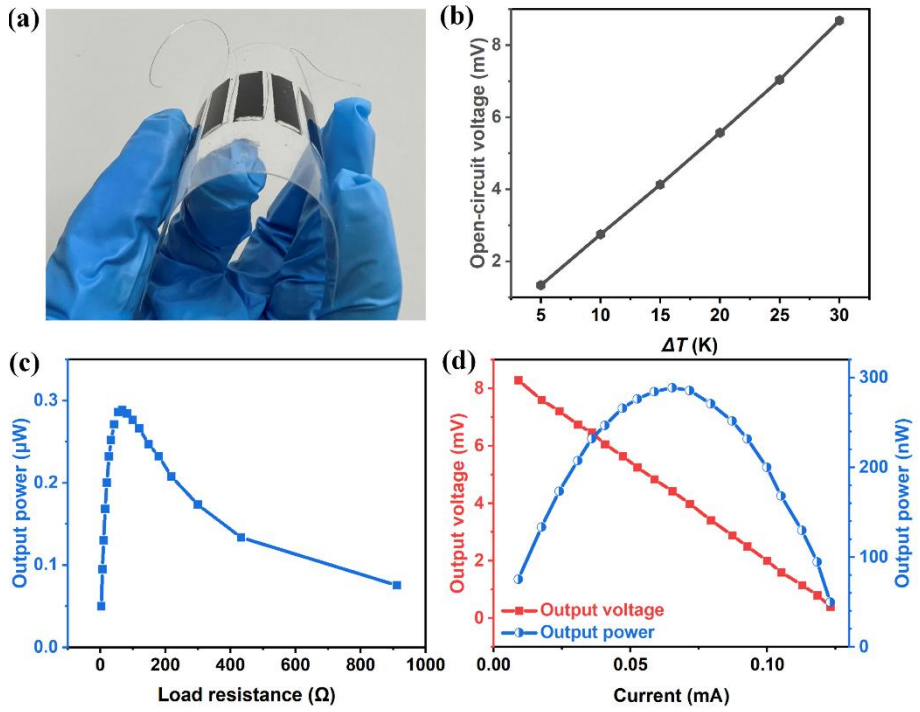

Fig. 4. (a) The photograph of fabricated flexible TE module; (b) Open-circuit voltage of the thermoelectric module as a function of temperature gradient; (c) Output power of the thermoelectric module as a function of load resistance with temperature gradient of 30 K; (d) Output voltage and power of the thermoelectric module as a function of current with temperature gradient of 30 K.

4. Conclusion

We put forward an effective strategy to improve the dispersion and thermoelectric properties of carbon nanotubes by green lignin, in which well-dispersed CNTs with uniform interconnected conductive networks were constructed to facilitate carrier transport. The presence of π-π interactions between carbon nanotubes and the aromatic ring structure of lignin, and electrostatic repulsion arising from the ionized group of lignin contribute to the improved CNTs dispersion with decreased bundle diameter. The

better dispersion reduces the energy barriers between CNTs junctions and facilitates carrier transfer, leading to improved electrical properties. Moreover, Seebeck coefficient was also synergistically increased due to the energy filtering effect between CNTs and lignin. Consequently, a maximum power factor of 198.0 μW $m^{-1}K^{-2}$ was obtained for 11.8 wt% CNTs/lignin film with the electrical conductivity and the Seebeck coefficient of 993 S cm^{-1} and 44.7 μV k^{-1}, respectively. Then, the composite film was further base treated to partially remove insulating lignin, leading to an enhanced PF of 223.1 μW m^{-1} K^{-2}, higher than most values of reported CNTs. Furthermore, the flexible TE device with five pairs of CNTs/lignin-A film (p-type) and nickel wire (n-type) could generate a high power of 288 nW at ΔT = 30 K, demonstrating the potential application of renewable lignin for sustainable energy utilization.

CRediT authorship contribution statement

Han Zhang: Investigation, Formal analysis, Writing – original draft. Hui Li: Supervision, Conceptualization, Formal analysis, Data curation, Writing – review & editing. Wenbo Wang: Investigation. Pengcheng Li: Supervision, Writing – review & editing. Siqi Liu: Formal analysis. Ming Yang: Formal analysis. Chaobin He: Supervision, Writing – review & editing.

Conflicts of interest

All authors declared that there are no conflicts of interest.

Acknowledgments

This work was supported by the National Natural Science Foundation of China

(Grant No. 51803156, 51903194), A*STAR Individual Research Grants (Grant No. M23M6c0107), Hubei Provincial Natural Science Foundation of China (2023AFB781), Youths Science Foundation of Wuhan Institute of Technology (No. K202228), Post-graduate Education Innovation Fund of Wuhan Institute of Technology (CX2023104), and Scientific Research Program of Hubei Provincial Department of Education (No. B2022059).

Appendix A. Supplementary data

Supplementary data to this article can be found online.

References

[1] S. Magina, A. Rudnitskaya, S. Soreto, L.C. Costa, A. Barros-Timmons, D.V. Evtuguin, Lignosulfonate-based conducting-flexible polymeric membranes for liquid sensing applications, Materials 14(18) (2021) 5331.

[2] H. Li, J.-T. Sun, C. Wang, S. Liu, D. Yuan, X. Zhou, et al., High modulus, strength, and toughness polyurethane elastomer based on unmodified lignin, ACS Sustainable Chem. Eng. 5(9) (2017) 7942-7949.

[3] M.A.S. Badri, N.F.a.M. Noor, A.R.M. Zain, M. MatSalleh, T.H.T.A. Aziz, Exfoliated graphene-alkaline lignin-PEDOT: PSS composite as a transparent conductive electrode, Nanomater. Nanotechnol. 11 (2021) 1847-9804.

[4] N.-Y. Teng, I. Dallmeyer, J.F. Kadla, Effect of softwood kraft lignin fractionation on the dispersion of multiwalled carbon nanotubes, Ind. Eng. Chem. Res. 52(19) (2013) 6311-6317.

[5] H. Li, Y. Liang, P. Li, C. He, Conversion of biomass lignin to high-value polyurethane: a review, J. Bioresour. Bioprod. 5(3) (2020) 163-179.

[6] H. Li, Y. Zhao, S. Liu, P. Li, D. Yuan, C. He, Hierarchical porous carbon monolith derived from lignin for high areal capacitance supercapacitors, Micropor. Mesopor. Mat. 297 (2020) 109960.

[7] D. Jiang, Y. Li, Z. Li, Z. Yang, Z. Xia, P. Fu, et al., High-Performance MoS2/SWCNT Composite Films for a Flexible Thermoelectric Power Generator, ACS Appl. Mater. Interfaces 15(25) (2023) 30495-30503.

[8] S. Liu, H. Li, P. Li, Y. Liu, C. He, Recent Advances in Polyaniline-Based Thermoelectric Composites, CCS Chem. 3(10) (2021) 2547-2560.

[9] N. Wen, Z. Fan, S. Yang, Y. Zhao, T. Cong, S. Xu, et al., Highly conductive, ultra-flexible and continuously processable PEDOT: PSS fibers with high thermoelectric properties for wearable energy harvesting, Nano Energy 78 (2020) 105361.

[10] H. Li, C. Zhang, P. Li, S. Liu, H. Zhang, C. He, Recent development in flexible organic thermoelectric fibers for wearable devices, Mater. Today Chem. 34 (2023) 101774.

[11] S.Q. Liu, H. Li, J.C.C. Yeo, J. Kong, P. Anukunwithaya, C.B. He, Solvent-optimized monolithic SWCNT-based thermoelectric generator for efficient electricity harvesting from body heat and sunlight, Carbon 203 (2023) 111-119.

[12] L. Wang, X. Zhang, L.D. Zhao, Evolving strategies toward Seebeck coefficient enhancement, Acc. Mater. Res. 4(5) (2023) 448-456.

[13] N. Wen, Z. Fan, S. Yang, Y. Zhao, C. Li, T. Cong, et al., High-performance

stretchable thermoelectric fibers for wearable electronics, Chem. Eng. J. 426 (2021) 130816.

[14] H. Lv, L. Liang, Y. Zhang, L. Deng, Z. Chen, Z. Liu, et al., A flexible spring-shaped architecture with optimized thermal design for wearable thermoelectric energy harvesting, Nano Energy 88 (2021) 106260.

[15] X.D. Wang, H. Wang, B. Liu, Carbon nanotube-based organic thermoelectric materials for energy harvesting, Polymers 10(11) (2018) 1196.

[16] S. Wei, L. Liu, X. Huang, Y. Zhang, F. Liu, L. Deng, et al., Flexible and foldable films of SWCNT thermoelectric composites and an S-shape thermoelectric generator with a vertical temperature gradient, ACS Appl. Mater. Interfaces 14(4) (2022) 5973-5982.

[17] R.X. A, H.S. A, S.N. B, Dispersing and doping carbon nanotubes by poly(p-styrene-sulfonic acid) for high-performance and stable transparent conductive films, Carbon 164 (2020) 150-156.

[18] S. Li, Y. Ci, D. Zhang, C. Zhang, Y. He, Free arc liquid-phase dispersion method for the preparation of carbon nanotube dispersion, Carbon Lett. 31(2) (2020) 287-295.

[19] A. Esmaeili, C. Sbarufatti, K. Youssef, A. Jiménez-Suárez, A. Ureña, A.M.S. Hamouda, Enhanced tensile strength, fracture toughness and piezoresistive performances of CNT based epoxy nanocomposites using toroidal stirring assisted ultra-sonication, Mech. Adv. Mater. Struc. 29(26) (2021) 5557-5566.

[20] S. Siljander, P. Keinänen, A. Räty, K. Ramakrishnan, S. Tuukkanen, V. Kunnari, et al., Effect of surfactant type and sonication energy on the electrical conductivity

properties of nanocellulose-CNT nanocomposite films, Int. J. Mol. Sci. 19(6) (2018) 1819.

[21] B. Krause, M. Mende, P. Pötschke, G. Petzold, Dispersability and particle size distribution of CNTs in an aqueous surfactant dispersion as a function of ultrasonic treatment time, Carbon 48(10) (2010) 2746-2754.

[22] Olga Matarredona, Heather Rhoads, Zhongrui Li, Jeffrey H. Harwell, Leandro Balzano, D.E. Resasco, Dispersion of single-walled carbon nanotubes in aqueous solutions of the anionic surfactant NaDDBS, J. Phys. Chem. B 107(48) (2014) 13251-13550.

[23] M.F. Islam, E. Rojas, D.M. Bergey, A.T. Johnson, A.G. Yodh, High weightfraction surfactant solubilization of single-wall carbon nanotubes in water, Nano Lett. 3(2) (2003) 260-283.

[24] D.D. Freeman, K. Choi, C. Yu, N-type thermoelectric performance of functionalized carbon nanotube-filled polymer composites, PLoS One 7(11) (2012) e47822.

[25] Y. Xu, Y. Tan, Y. Xue, M. Pei, D. Zhang, S. Liu, et al., A novel PVA/MWCNTs hydrogel with high toughness and electromagnetic shielding properties, Polym. Eng. Sci. 63(11) (2023) 3555-3564.

[26] Y. Liu, L. Gao, S. Zheng, Y. Wang, J. Sun, H. Kajiura, et al., Debundling of single-walled carbon nanotubes by using natural polyelectrolytes, Nanotechnology 18(36) (2007) 365702.

[27] H. Li, Y. Liu, S. Liu, P. Li, C. Zhang, C. He, Wet-spun flexible carbon

nanotubes/polyaniline fibers for wearable thermoelectric energy harvesting, Compos Part A: Appl S. 166 (2023) 107386.

[28] H. Li, Y. Liang, Y. Liu, S. Liu, P. Li, C. He, Engineering doping level for enhanced thermoelectric performance of carbon nanotubes/polyaniline composites, Compos. Sci. Technol. 210 (2021) 108797.

[29] C. Zhang, H. Li, Y. Liu, P. Li, S. Liu, C. He, Advancement of polyaniline/carbon nanotubes based thermoelectric composites, Materials 15(23) (2022) 8644.

[30] R. Tang, S. Yang, P. Li, H. Zhang, H. Li, Z. Liu, Enhancing thermoelectric performance of single-walled carbon nanotube films by poly(styrene sulfonate acid) dispersing and sequential base treatment, Compos. Commun. 47 (2024) 101873.

[31] Y.F. Jiang, H. Song, R. Xu, Research on the dispersion of carbon nanotubes by ultrasonic oscillation, surfactant and centrifugation respectively and fiscal policies for its industrial development, Ultrason. Sonochem. 48 (2018) 30-38.

[32] W. Dai, J. Wang, X. Gan, H. Wang, X. Su, C. Xi, A systematic investigation of dispersion concentration and particle size distribution of multi-wall carbon nanotubes in aqueous solutions of various dispersants, Colloid Surface A. 589 (2020) 124369.

[33] A. Zarebidaki, S.-R. Allahkaram, Effect of surfactant on the fabrication and characterization of Ni-P-CNT composite coatings, J. Alloys Compd. 509(5) (2011) 1836-1840.

[34] G. Milczarek, M. Nowicki, Carbon nanotubes/kraft lignin composite: Characterization and charge storage properties, Mater. Res. Bull. 48(10) (2013) 4032-4038.

[35] G. Milczarek, Kraft lignin as dispersing agent for carbon nanotubes, J. Electroanal. Chem. 638(1) (2010) 178-181.

[36] Sheila M. Goodman, N. Ferguson, A.B. Dichiara, Lignin-assisted double acoustic irradiation for concentrated aqueous dispersions of carbon nanotubes, RSC Adv. 7(9) (2017) 5488-5496.

[37] W. Liu, R. Zhou, D. Zhou, G. Ding, J.M. Soah, C.Y. Yue, et al., Lignin-assisted direct exfoliation of graphite to graphene in aqueous media and its application in polymer composites, Carbon 83 (2015) 188-197.

[38] M. Culebras, G. Ren, S. O'Connell, J.J. Vilatela, M.N. Collins, Lignin doped darbon nanotube yarns for improved thermoelectric efficiency, Adv. Sustain. Syst. 4(11) (2020) 2000147.

[39] W. Liu, R. Zhou, H.L.S. Goh, S. Huang, X. Lu, From waste to functional additive: toughening epoxy resin with lignin, ACS Appl. Mater. Interfaces 6(8) (2014) 5810-5817.

[40] H. Li, Y. Liu, P. Li, S. Liu, F. Du, C. He, Enhanced thermoelectric performance of carbon nanotubes/polyaniline composites by multiple interface engineering, ACS Appl. Mater. Interfaces 13(5) (2021) 6650-6658.

[41] S. Qu, M. Wang, Y. Chen, Q. Yao, L. Chen, Enhanced thermoelectric performance of CNT/P3HT composites with low CNT content, RSC Adv. 8(59) (2018) 33855-33863.

[42] T.H. Kim, J.S. Kim, C. Sunwoo, Y.Y. Lee, Pretreatment of corn stover by aqueous ammonia, Bioresour. Technol. 90(1) (2003) 39-47.

[43] P.L. Tang, O. Hassan, C.S. Yue, P.M. Abdul, Lignin extraction from oil palm empty

fruit bunch fiber (OPEFBF) via different alkaline treatments, Biomass. Convers. Bior. 10(1) (2019) 125-138.

[44] J. Lisperguer, P. Perez, U. S., Structure and thermal properties of lignins: characterization by infrared spectroscopy and differential scanning calorimetry, J. Chil. Chem. Soc. 54(4) (2009) 460-463.

[45] L. Hu, D.S. Hecht, G. Grüner, Infrared transparent carbon nanotube thin films, Appl. Phys. Lett. 94(8) (2009) 1273.

[46] K. Zhu, Z. Hu, G. Chen, Enhancement of thermoelectric property of carbon nanotubes by p-type doping with judicious molecular design of spiro-bifluorene derivatives, Compos. Commun. 32 (2022) 101166.

[47] G. Cao, G. He, L. Lu, Q. Zhang, Y. Yan, X. Tang, et al., Hydrogen-bonded n-type waterborne polyurethane/lysine/single-walled carbon nanotube ternary composite: Combining excellent thermoelectric and stretchable properties toward self-powered temperature and strain sensors, Chem. Eng. J. 474 (2023) 145664.

[48] Q. Meng, L. Zhao, Y. Geng, P. Yin, Z. Mao, X. Sui, et al., A one-pot approach to prepare stretchable and conductive regenerated silk fibroin/CNT films as multifunctional sensors, Nanoscale 15(21) (2023) 9403-9412.

[49] S. Liu, H. Li, C. He, Simultaneous enhancement of electrical conductivity and seebeck coefficient in organic thermoelectric SWNT/PEDOT:PSS nanocomposites, Carbon 149 (2019) 25-32.

[50] L. Jiang, L. Gao, J. Sun, Production of aqueous colloidal dispersions of carbon nanotubes, J. Colloid Interface Sci. 260(1) (2003) 89-94.

[51] H.-Q. Ye, Y.-H. Deng, Y. Yan, M.-J. Zhang, Y. Qian, X.-Q. Qiu, Influence of soldium lignosulfonate with different molecular weights on the dispersion of multiwalled carbon nanotubes, Acta Phys. -Chim. Sin. 31(10) (2015) 1991-1996.

[52] R.A. Lee, C. Bédard, V. Berberi, R. Beauchet, J.-M. Lavoie, UV–Vis as quantification tool for solubilized lignin following a single-shot steam process, Bioresour. Technol. 144 (2013) 658-663.

[53] L. Wang, Q. Yao, W. Shi, S. Qu, L. Chen, Engineering carrier scattering at the interfaces in polyaniline based nanocomposites for high thermoelectric performances, Mater. Chem. Front. 1(4) (2017) 741-748.

[54] Y. Wang, C. Yu, M. Sheng, S. Song, Y. Deng, Individual Adjustment of Electrical Conductivity and Thermopower Enabled by Multiple Interfaces in Polyaniline-Based Ternary Hybrid Nanomaterials for High Thermoelectric Performances, Adv. Mater. Interfaces 5(10) (2018) 1701168.

[55] S. Liu, H. Li, C. He, Simultaneous enhancement of electrical conductivity and seebeck coefficient in organic thermoelectric SWNT/PEDOT: PSS nanocomposites, Carbon 149 (2019) 25-32.

[56] S. Qu, Q. Yao, L. Wang, J. Hua, L. Chen, A novel hydrophilic pyridinium salt polymer/SWCNTs composite film for high thermoelectric performance, Polymer 136 (2018) 149-156.

[57] O.I. Akinboye, Y. Zhang, V.K.R. Kondapalli, F. Yang, V. Mandrolko, M. Isaiev, et al., Boosting Thermoelectric Power Factor of Carbon Nanotube Networks with Excluded Volume by Co-Embedded Microparticles, ACS Appl. Mater. Interfaces 15(36)

(2023) 42881-42890.

[58] M. Gnanaseelan, Y. Chen, J.J. Luo, B. Krause, J. Pionteck, P. Pötschke, et al., Cellulose-carbon nanotube composite aerogels as novel thermoelectric materials, Compos. Sci. Technol. 163 (2018) 133-140.

[59] A.J. Paleo, Y. Martinez-Rubi, B. Krause, P. Pötschke, M.B. Jakubinek, B. Ashrafi, et al., Carbon Nanotube–Polyurethane Composite Sheets for Flexible Thermoelectric Materials, ACS Appl. Nano Mater. 6(19) (2023) 17986-17995.

[60] M. Zhang, X. Cao, M. Wen, C. Chen, Q. Wen, Q. Fu, et al., Highly Electrical Conductive PEDOT:PSS/SWCNT Flexible Thermoelectric Films Fabricated by a High-Velocity Non-solvent Turbulent Secondary Doping Approach, ACS Appl. Mater. Interfaces 15(8) (2023) 10947-10957.

[61] Z. Saadi, S.G. King, J.V. Anguita, V. Stolojan, S.R.P. Silva, Effect of surfactants on the thermoelectric performance of double-walled carbon nanotubes, Energy Environ. Mater. 6(1) (2022) e12281.

[62] S. Hata, H. Le Thu Thao, H. Ihara, Y. Du, Y. Shiraishi, N. Toshima, n-Type thermoelectric behavior in oxyethylene surfactant/carbon nanotubes, Energy Adv. 2(1) (2023) 86-90.

[63] D.E. Choi, J. Im, Y. Ahn, K. Hwang, J. Kim, J.E. Kwon, et al., Sequential Doping of Carbon Nanotube Wrapped by Conjugated Polymer for Highly Conductive Platform and Thermoelectric Application, Small Struct. 5(1) (2023) 2300321.

[64] Z.T. Liu, Y.C. Hu, P.C. Li, J. Wen, J.G. He, X. Gao, Enhancement of Thermoelectric Performance of DPP based Polymer by Introducing 3,4-

Ethylenedioxythiophene Electron-rich Building Block., J. Mater. Chem. C 8(31) (2020) 10859-10867.

[65] Y. Wang, Q. Li, J. Wang, Z. Li, K. Li, X. Dai, et al., Understanding the solvent effects on polarity switching and thermoelectric properties changing of solution-processable n-type single-walled carbon nanotube films, Nano Energy 93 (2022) 106804.

[66] Y. Qin, Q. Wang, L.M. Wang, The synergic regulation of conductivity and Seebeck coefficient in pure polyaniline by chemically changing the ordered degree of molecular chains., J. Mater. Chem. A 2(8) (2014) 2634-2640.

[67] Y. Cho, N. Okamoto, S. Yamamoto, S. Obokata, K. Nishioka, H. Benten, et al., Carbon nanotube/biomolecule composite yarn for wearable thermoelectric applications, ACS Appl. Energy Mater. 5(3) (2022) 3698-3705.

[68] H.B. Li, Y.D. Zong, Q.J. Ding, W.J. Han, X. Li, Paper-based thermoelectric generator based on multi-walled carbon nanotube/carboxylated nanocellulose, J. Power Sources 500 (2021) 229992.

[69] G. Cao, G. He, L. Lu, Q. Zhang, Y. Yan, X. Tang, et al., Hydrogen-bonded n-type waterborne polyurethane/lysine/single-walled carbon nanotube ternary composite: Combining excellent thermoelectric and stretchable properties toward self-powered temperature and strain sensors, Chem. Eng. J 474 (2023) 145664.